A Mixed Hybrid Mortar Method for solving flow in Discrete Fracture Networks

G. Pichot[a**] and J. Erhel[b] and J. R. de Dreuzy [a]
[a] *CNRS, UMR6118, Géosciences Rennes, France*; [b] *Inria Rennes, France*

Abstract

We consider flow in Discrete Fracture Networks made of 2D domains in intersection and solved with a Mixed Hybrid Finite Element Method (MHFEM). The discretization within each fracture is performed in two steps: first, borders and intersections are discretized, second, based on these discretizations, a 2D mesh is built. Independent meshing process within each subdomain is of interest for practical use since it makes it easier to refine the chosen subdomains and to perform parallel computation. This paper shows how MHFEM is well adapted for integrating a Mortar method to enforce the continuity of the fluxes and heads at the non-matching grids. Some numerical simulations are given to show the efficiency of the method in the case of a preferential orientation of the fractures where a comparison with the 2D solution is possible.

Keywords: Mixed Hybrid Finite Element Method; Mortar method; Fractured media;

AMS Subject Classifications: 65N30, 65N55, 65N22

1 Introduction

Studying flow in fractured networks is of interest for many applications from water resources to pollutant dissemination and oil prospecting. The major difficulty of such a medium is its heterogeneity at various scales. A classical approach is to generate Discrete Fracture Networks (DFNs) and to simulate flow through the fractures. Fractures are commonly modeled as 2D domains whose parameters follow given probability distributions so as to take uncertainty into account [1]. Intensive numerical simulations with various configurations of DFNs are then required for upscaling the permeability as well as the flow organization.

**Corresponding author. Email: geraldine.pichot@univ-rennes1.fr

Suppose a stochastic DFN is generated. Let us consider steady-state flow and assume that the rock matrix is impervious; we also assume that there is no longitudinal flow in the intersections between fractures. Thus, physical model is governed by Poiseuille's law and mass conservation in each fracture, with continuity of hydraulic head and of transversal flux in each intersection. Spatial discretization is necessary to solve the partial differential equations. Finite Element methods make it easier to deal with irregular geometries by using a triangular mesh in 2D domains. However, DFNs are complex 3D structures with 2D domains intersecting each other. A challenge comes with the meshing of such networks, where the mesh must be of good quality and must not contain too many cells. In [2], a method to generate a mesh of good quality has been developed. It is based on a conforming discretization of intersections, in the sense that each intersection has a unique 3D discrete representation. It also relies on a unique mesh step for all fractures. However, the number of cells can be large, especially if the network contains large fractures as well as small fractures.

This paper addresses this difficulty by introducing non-matching discretizations of intersections. The idea is to generate a 2D mesh in each fracture with possibly different mesh steps from one fracture to another and to apply interface conditions using a mortar method. The mortar method was born with the works of Bernardi et al. [3], [4] to connect subdomains with finite elements on one side and spectral elements on the other side. Next it has known a spectacular growth as it is attested by the amount of publications (see the references in [5]). It is also widely used to deal with non-matching grids between subdomains. Especially, it has been studied in details by Arbogast et al. [6].

We use a mixed hybrid finite element method which allows to eliminate the flux unknowns and to consider a system with only trace of hydraulic head unknowns and mean hydraulic head unknowns [2], [7], [8], [9] . It appears that this method is well adapted for integrating a mortar method.

In section 2, we recall the physical model, with the geometry and the equations. In section 3, we recall the formulation of a mixed hybrid finite element method applied to fractured media in the matching grids case. This is the basis of our method in 3D networks. In section 4, we describe our mortar method applied to 3D fracture networks with non-matching grids and the assumption that intersections do not cross nor overlap. Interface conditions are written by defining master intersection sides along with slave intersection sides. We derive the algebraic form of these conditions as well as the algebraic form of laws in each domain. It is then possible to eliminate flux unknown as in the classical mixed hybrid approach and to get a system with only trace of hydraulic head at edges of the mesh and mean hydraulic head. We show good properties of the matrix of the system. In section 5, we apply our mortar method and compare it with the method using matching grids. We use an example of network where a comparison with a corresponding 2D solution is possible. Results show a fairly good accuracy of the mortar method.

2 Governing equations

Consider a cubic domain where there are N_f intersecting fractures that form a computational domain Ω. The boundary of Ω is composed of the borders of the fractures, which may be truncated by the edges of the cube (Figure 1).

We use the following notations within each fracture f:

- We denote by Ω_f the f-th fracture domain less the intersection, $f = 1, ..., N_f$, $\partial\Omega_f = \Gamma_f \cup \Sigma_f$;
- Let Γ_f be the border of the fracture f (which may be truncated by the edges of the cube);
- Let Σ_f be the set of all intersections within the fracture f (for the sake of simplicity in the writing of the mathematical part, we assume that $meas(\Gamma_f \cap \Sigma_f) = 0$);

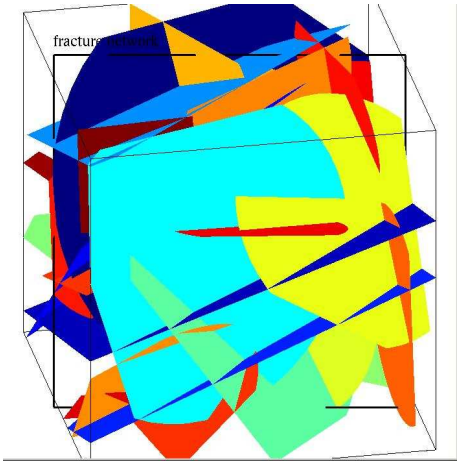

Figure 1: Example of a domain with 30 fractures in intersections

Classical laws governing the flux, mass conservation and Poiseuille's law, are assumed in each fracture and there are also conditions at the intersections of fractures: continuity of the hydraulic head and of the transversal flux at each intersection. We assume there is no longitudinal flux within the intersections. See [10] for equations in case of a non null longitudinal flux in the intersections.

Boundary conditions are imposed on the cube edges. Let us denote by Γ_N the boundaries of the cube with Neumann boundary conditions and Γ_D the ones with Dirichlet boundary conditions ($\Gamma_D \neq 0$). Recall the rock matrix is supposed impervious so for each fracture f, one imposes a homogeneous Neumann Boundary condition on $\Gamma_f \backslash \{(\Gamma_f \cap \Gamma_D) \cup (\Gamma_f \cap \Gamma_N)\}$.

Let N_i be the number of intersections of fractures. Let us denote by Σ_k the k-th intersection, $k = 1, ..., N_i$, and F_k the set of fractures with Σ_k on the boundary.

Consider the coordinates $\mathbf{x} = (x, y)$, local to the fracture f. For the unknown hydraulic head scalar function $p(\mathbf{x})$ and the flux per unit length function $\mathbf{u}(\mathbf{x})$ (corresponding to the velocity multiplied by the aperture of the fracture), we have:

$$\nabla \cdot \mathbf{u}(\mathbf{x}) = \mathbf{f}(\mathbf{x}), \qquad \text{for } \mathbf{x} \in \Omega_f, \tag{1a}$$
$$\mathbf{u}(\mathbf{x}) = -\mathcal{T}(\mathbf{x})\nabla p(\mathbf{x}), \qquad \text{for } \mathbf{x} \in \Omega_f, \tag{1b}$$
$$p(\mathbf{x}) = p^D(\mathbf{x}), \qquad \text{on } \Gamma_D \cap \Gamma_f, \tag{1c}$$
$$\mathbf{u}(\mathbf{x}).\boldsymbol{\nu} = q^N(\mathbf{x}), \qquad \text{on } \Gamma_N \cap \Gamma_f, \tag{1d}$$
$$\mathbf{u}(\mathbf{x}).\boldsymbol{\mu} = \mathbf{0}, \qquad \text{on } \Gamma_f \backslash \{(\Gamma_f \cap \Gamma_D) \cup (\Gamma_f \cap \Gamma_N)\}, \tag{1e}$$

where $\boldsymbol{\nu}$ (respectively $\boldsymbol{\mu}$) denotes the outward normal unit vector of the border $\Gamma_N \cap \Gamma_f$ (respectively $\Gamma_f \backslash \{(\Gamma_f \cap \Gamma_D) \cup (\Gamma_f \cap \Gamma_N)\}$) with respect to the fracture f. The parameter $\mathcal{T}(\mathbf{x})$ is a given transmissivity field (unit $[\mathrm{m}^2.\mathrm{s}^{-1}]$). The function $\mathbf{f}(\mathbf{x}) \in L^2(\Omega_f)$ represents the sources/sinks.

Continuity conditions in each intersection are written as [2], [11]:

$$p_{k,f} = p_k, \qquad \text{on } \Sigma_k, \forall f \in F_k, \tag{2a}$$
$$\sum_{f \in F_k} \mathbf{u}_{k,f}.\mathbf{n}_{k,f} = 0, \qquad \text{on } \Sigma_k, \tag{2b}$$

where $p_{k,f}$ is the trace of hydraulic head on Σ_k in the fracture f, p_k is the unknown hydraulic head on the intersection Σ_k and $\mathbf{u}_{k,f}.\mathbf{n}_{k,f}$ is the normal flux through Σ_k coming from the fracture Ω_f, with $\mathbf{n}_{k,f}$ the outward normal unit vector of the intersection Σ_k with respect to the fracture Ω_f. Equations $(2a) - (2b)$ express the continuity of p and the mass balance of $\mathbf{u}$ across the intersections between fractures (what is the outflow from one fracture must be the inflow into the neighboring ones).

3 Matching grids and mixed hybrid formulation

Let us first recall the mixed hybrid weak formulation for fractured media in case of matching grids at the fracture intersections. We assume $(1a-1e)$ hold within each fracture, together with the additional continuity conditions $(2a - 2b)$ at each intersection.

The boundary of Ω and the set of all intersections $\cup_{f=1}^{N_f} \Sigma_f$ are discretized at first, with matching grids at the intersections. Based on these discretizations, each fracture Ω_f is meshed with triangular elements, to form a 2D mesh $\mathcal{T}_{h,f}$. The total mesh is called $\mathcal{T}_h = \cup_{f=1}^{N_f} \mathcal{T}_{h,f}$.

We define:

- $\mathcal{E}_{h,f,in}$: "inner" edges in $\Omega_f \cup \Gamma_f$;
- $\mathcal{E}_{h,f,\Sigma}$: intersection edges in Σ_f;
- $\mathcal{E}_{h,\Sigma} = \cup_{f=1}^{N_f} \mathcal{E}_{h,f,\Sigma}$: all intersection edges;
- $\mathcal{E}_{h,in} : \cup_{f=1}^{N_f} \mathcal{E}_{h,f,in}$: all inner edges;
- $\mathcal{E}_{h,f} = \mathcal{E}_{h,f,in} \cup \mathcal{E}_{h,f,\Sigma}$: all edges within the fracture f;
- $\mathcal{E}_h = \cup_{f=1}^{N_f} \mathcal{E}_{h,f}$: all edges;
- $\mathcal{E}_{h,D} = \{E \in \mathcal{E}_h, E \in \Gamma_D\}$ and $\mathcal{E}_{h,N} = \{E \in \mathcal{E}_h, E \in \Gamma_N\}$.

Define the Raviart-Thomas (RT) spaces, for $K \in \mathcal{T}_h$:

$$\begin{aligned} &RT^0(K) = \{s \in (P_1(K))^2 \text{ such that } s = (a + b\,x,\, c + b\,y), a, b, c \in \mathbb{R}\} \\ &RT^0(\mathcal{T}_{h,f}) = \{\phi \in L^2(\Omega_f) \text{ such that } \phi|_K \in RT^0(K), \forall K \in \mathcal{T}_{h,f}\} \end{aligned} \tag{3}$$

where $P_d(K)$ denotes the space of polynomials of total degree d defined on K.

One also needs a space $\mathcal{M}^0(\mathcal{T}_{h,f})$ defined as:

$$\mathcal{M}^0(\mathcal{T}_{h,f}) = \{\varphi \in L^2(\Omega_f) \text{ such that } \varphi|_K \in P_0(K), \forall K \in \mathcal{T}_{h,f}\} \tag{4}$$

3.1 Discrete mixed hybrid weak formulation

Within each fracture f, we look for $\mathbf{u}_{h,f}$ in the space $RT^0(\mathcal{T}_{h,f})$. The hydraulic head in the fracture f is approximated by a piecewise constant function $p_{h,f}$ in $\mathcal{M}^0(\mathcal{T}_{h,f})$.

We define the space $\mathcal{N}^0(\mathcal{E}_{h,f})$ of functions constant on edges in $\mathcal{E}_{h,f}$.

$$\begin{aligned} &\mathcal{N}^0(\mathcal{E}_{h,f}) = \{\mu_h \in L^2(\mathcal{E}_{h,f}) \text{ such that } \mu_h|_E \in P_0(E),\ \forall E \in \mathcal{E}_{h,f}\} \\ &\mathcal{N}^0_{p^D,D}(\mathcal{E}_{h,f}) = \{\mu_h \in \mathcal{N}^0(\mathcal{E}_{h,f}) \text{ such that } \int_E (\mu_h - p^D) dl = 0,\ \forall E \in \mathcal{E}_{h,D} \cap \mathcal{E}_{h,f}\}. \end{aligned} \tag{5}$$

If $p^D \equiv 0$ on $\Gamma_D \cap \Gamma_f$, we obtain the space $\mathcal{N}^0_{0,D}(\mathcal{E}_{h,f})$.

One also needs to define:

$$\begin{aligned}
&\mathcal{N}^0(\mathcal{E}_h) = \{\mu_h \in L^2(\mathcal{E}_h) \text{ such that } \mu_h|_E \in P_0(E),\ \forall E \in \mathcal{E}_h\}\\
&\mathcal{N}^0(\mathcal{E}_{h,\Sigma}) = \{\mu_h \in \mathcal{N}^0(\mathcal{E}_h) \text{ such that } \mu_h|_E = 0,\ \forall E \notin \mathcal{E}_{h,\Sigma}\}\\
&\mathcal{N}^0(\mathcal{E}_{h,f,\Sigma}) = \{\mu_h \in \mathcal{N}^0(\mathcal{E}_{h,f}) \text{ such that } \mu_h|_E = 0,\ \forall E \notin \mathcal{E}_{h,f,\Sigma}\}\\
&\mathcal{N}^0_{0,D}(\mathcal{E}_{h,f,in}) = \{\mu_h \in \mathcal{N}^0_{0,D}(\mathcal{E}_{h,f}) \text{ such that } \mu_h|_E = 0,\ \forall E \notin \mathcal{E}_{h,f,in}\}.
\end{aligned} \tag{6}$$

A new degree of freedom $\lambda_{h,f}$ is introduced that approximates, in the fracture f, the traces of hydraulic head on the edges of the mesh $\mathcal{T}_{h,f}$. We also consider the unknown $\lambda_\Sigma \in \mathcal{N}^0(\mathcal{E}_{h,\Sigma})$ that approximates the traces of hydraulic head on the intersections Σ. This allows to consider the general case where an intersection edge may involve a varying number of fractures. The discrete mixed hybrid weak formulation reads as:

For each fracture f,

Find $(\mathbf{u}_{h,f}, p_{h,f}, \lambda_{h,f}) \in RT^0(\mathcal{T}_{h,f})$ x $\mathcal{M}^0(\mathcal{T}_{h,f})$ x $\mathcal{N}^0_{p^D,D}(\mathcal{E}_{h,f})$ such that:

$$\sum_{K\in\mathcal{T}_{h,f}} \left(\int_K \mathcal{T}^{-1}\mathbf{u}_{h,f}.\boldsymbol{\chi}_{h,f} d\mathbf{x} + \int_{\partial K} \lambda_{h,f}\boldsymbol{\chi}_{h,f}.\boldsymbol{\nu}_{K,f} dl - \int_K p_{h,f}\nabla\cdot\boldsymbol{\chi}_{h,f} d\mathbf{x} \right) = 0,$$

$$\forall \boldsymbol{\chi}_{h,f} \in RT^0(\mathcal{T}_{h,f}), \tag{7a}$$

$$\sum_{K\in\mathcal{T}_{h,f}} \left(\int_K \nabla\cdot\mathbf{u}_{h,f}.\varphi_{h,f} d\mathbf{x} - \int_K f\varphi_{h,f} d\mathbf{x} \right) = 0, \forall \varphi_{h,f} \in \mathcal{M}^0(\mathcal{T}_{h,f}), \tag{7b}$$

$$\sum_{K\in\mathcal{T}_{h,f}} \left(\int_{\partial K} \mathbf{u}_{h,f}.\boldsymbol{\nu}_{K,f}\mu_{h,f} dl - \int_{\partial K\cap\Gamma_N} q^N\mu_{h,f} dl \right) = 0,\ \forall \mu_{h,f} \in \mathcal{N}^0_{0,D}(\mathcal{E}_{h,f,in}), \tag{7c}$$

$$\sum_{f=1}^{N_f} \sum_{K\in\mathcal{T}_{h,f}} \left(\int_{\partial K} \mathbf{u}_{h,f}.\boldsymbol{\nu}_{K,f}\mu_{h,\Sigma} dl \right) = 0,\ \forall \mu_{h,\Sigma} \in \mathcal{N}^0(\mathcal{E}_{h,\Sigma}), \tag{8a}$$

Find $\lambda_\Sigma \in \mathcal{N}^0(\mathcal{E}_{h,\Sigma})$ such that,
for each fracture f,

$$\int_{\Sigma_f} \lambda_{h,f}\mu_{h,\Sigma} dl = \int_{\Sigma_f} \lambda_\Sigma\mu_{h,\Sigma} dl,\ \forall \mu_{h,\Sigma} \in \mathcal{N}^0(\mathcal{E}_{h,f,\Sigma}), \tag{8b}$$

with $\boldsymbol{\nu}_{K,f}$ the outward normal unit vector to the considered border ∂K of the element K in $\mathcal{T}_{h,f}$.

Equation (7*c*) expresses the continuity of the normal component of $\mathbf{u}_{h,f}$ across the interelement boundaries.

Equations ($8a$) and ($8b$) are valid in the matching grids case. Equation ($8a$) imposes the continuity of the flux at the intersections and equation ($8b$) the continuity of the hydraulic head at the intersections. It should be noted that an intersection edge may belong to more than 2 fractures.

3.2 Global basis functions

The finite dimensional space $RT^0(\mathcal{T}_{h,f})$ is spanned by linearly independent vector basis functions $\mathbf{w}_{K,E_i}$, $i = 1,2,3$, $E_i \in \partial K$, $K \in \mathcal{T}_{h,f}$, such that $supp(\mathbf{w}_{K,E_i}) \subseteq K$ and

$$\int_{E_j} \mathbf{w}_{K,E_i}.\boldsymbol{\nu}_{K,E_j} dl = \delta_{E_i,E_j},\ E_i, E_j \subset \partial K. \tag{9}$$

A function $\mathbf{u}_{h,f} \in RT^0(\mathcal{T}_{h,f})$ has three degrees of freedom per element which are the fluxes across the element edges:

$$\mathbf{u}_{h,f} = \sum_{K \in \mathcal{T}_h} \sum_{E_i \subset \partial K, i=1,2,3} q_{K,E_i} \mathbf{w}_{K,E_i}. \tag{10}$$

The two spaces $\mathcal{M}^0(\mathcal{T}_{h,f})$ and $\mathcal{N}^0(\mathcal{E}_h)$ are spanned, respectively, by linearly independent scalar basis functions φ_K, $K \in \mathcal{T}_{h,f}$ and μ_E, $E \in \mathcal{E}_h$, such that

$$\begin{aligned} &\varphi_K = \delta_{K,K'},\ K, K^{'} \in \mathcal{T}_{h,f}, \\ &\mu_E = \delta_{E,E'},\ E, E^{'} \in \mathcal{E}_h. \end{aligned} \tag{11}$$

The hydraulic head $p_{h,f} \in \mathcal{M}^0(\mathcal{T}_{h,f})$ has one degree of freedom $p_{K,f}$ per element $K \in \mathcal{T}_{h,f}$, $\lambda_{h,f} \in \mathcal{N}^0_{p^D,D}(\mathcal{E}_{h,f})$ has one degree of freedom $\lambda_{E,f}$ per edge $E \in \mathcal{E}_{h,f}$ and $\lambda_\Sigma \in \mathcal{N}^0(\mathcal{E}_{h,\Sigma})$ has one degree of freedom $\lambda_{E,m}$ per edge $E \in \mathcal{E}_{h,\Sigma}$ such that:

$$\begin{aligned} p_{h,f} &= \sum_{K \in \mathcal{T}_{h,f}} p_{K,f} \varphi_K, \\ \lambda_{h,f} &= \sum_{E \in \mathcal{E}_{h,f}} \lambda_{E,f} \mu_E, \\ \lambda_\Sigma &= \sum_{E \in \mathcal{E}_{h,\Sigma}} \lambda_{E,m} \mu_E. \end{aligned} \tag{12}$$

3.3 Derivation of the linear system

Here we follow the methodology presented in [2] and [7].

We denote by $\mathbf{P_f}$ the vector of cell hydraulic head for all K in $\mathcal{T}_{h,f}$, by $\mathbf{\Lambda_f} = (\lambda_{\mathbf{E},\mathbf{f}})_{\mathbf{E} \in \mathcal{E}_{\mathbf{h},\mathbf{f}}}$ the vector of trace of hydraulic head unknowns on edges in $\mathcal{E}_{h,f}$ and by $\mathbf{\Lambda_m} = (\lambda_{\mathbf{E},\mathbf{m}})_{\mathbf{E} \in \mathcal{E}_{\mathbf{h},\mathbf{\Sigma}}}$ the vector of additional unknowns on intersection edges (edges in $\mathcal{E}_{h,\Sigma}$).

The vector Λ_f contains the trace of hydraulic head unknowns for the inner edges $\mathbf{\Lambda_{in,f}} = (\lambda_{\mathbf{E,f}})_{\mathbf{E}\in\mathcal{E}_{\mathbf{h,f,in}}}$ and for the intersection edges $\mathbf{\Lambda_{m,f}} = (\lambda_{\mathbf{E,f}})_{\mathbf{E}\in\mathcal{E}_{\mathbf{h,f,\Sigma}}}$ in the fracture f:

$$\mathbf{\Lambda_f} = \begin{pmatrix} \mathbf{\Lambda_{in,f}} \\ \mathbf{\Lambda_{m,f}} \end{pmatrix}. \tag{13}$$

We introduce $\mathbf{\Lambda_{in}} = (\mathbf{\Lambda_{in,f}})_\mathbf{f}$, the vector containing all trace of hydraulic head unknowns on inner edges within the system and $\mathbf{P} = (\mathbf{P_f})_\mathbf{f}$ the vector containing all mean hydraulic head unknowns in the system.

It is well known [7] that, locally on each triangle K in $\mathcal{T}_{h,f}$, the equation $(7a)$ leads to:

$$\mathbf{B_K Q_K} = p_{K,f}\mathbf{e} - \mathbf{\Lambda_K}, \tag{14}$$

with $\mathbf{Q_K}$ and $\mathbf{\Lambda}_K$ three dimensional vectors containing respectively the fluxes $q_{K,E_i}, i = 1,2,3$ and the traces of hydraulic head $\lambda_{E_i,f}, i = 1,2,3$ on each $E_i \subset \partial K$, and $\mathbf{e} = \begin{pmatrix} 1 & 1 & 1 \end{pmatrix}^T$.

We assume that the local transmissivity $\mathcal{T}_K$ is symmetric positive definite. Then the matrix $\mathbf{B_K}$ is a 3x3 symmetric positive definite matrix with elements:

$$(\mathbf{B_K})_{E_i,E_j} = \int_K \mathbf{w}_{K,E_i} \mathcal{T}_K^{-1} \mathbf{w}_{K,E_j} d\mathbf{x}. \tag{15}$$

We define $Q_{E,f}$ the jump of flux through the edge E in the fracture f by:

$$Q_{E,f} = \sum_{K\in\mathcal{T}_{h,f}, \partial K \supset E} q_{K,E}. \tag{16}$$

We have from $(7c)$ the relation [7]:

$$Q_{E,f} = \begin{cases} 0, \text{ if } E \in \mathcal{E}_{h,f,in} \backslash \Gamma_N \\ \\ q_E^N, \text{ if } E \in \Gamma_N. \end{cases} \tag{17}$$

On the intersections, the conditions to apply (corresponding to $(8a)$ and $(8b)$ respectively) are:

$$\forall E \in \mathcal{E}_{h,\Sigma}, \sum_f Q_{E,f} = 0, \tag{18a}$$

$$\lambda_{E,f} = \lambda_{E,m}, \forall f, \forall E \in \mathcal{E}_{h,f,\Sigma}, \tag{18b}$$

The condition $(18b)$ allows to substitute $\mathbf{\Lambda_{m,f}}$ by $\mathbf{\Lambda_m}$. We can now write the equations with $\mathbf{P}$, $\mathbf{\Lambda_{in}}$ and $\mathbf{\Lambda_m}$.

Using $(18b)$ and inverting the matrix $\mathbf{B_K}$ in (14), the mass conservation equations $(7b)$ write:

$$\mathbf{D}\,\mathbf{P} - \begin{pmatrix} \mathbf{R_{in}} & \mathbf{R_m} \end{pmatrix} \begin{pmatrix} \mathbf{\Lambda_{in}} \\ \mathbf{\Lambda_m} \end{pmatrix} = \mathbf{F}, \tag{19}$$

where $\mathbf{D}$ is a $card(\mathcal{T}_h)$x$card(\mathcal{T}_h)$ diagonal matrix and $\mathbf{F}$ is a vector of dimension $card(\mathcal{T}_h)$, which corresponds to the source/sink function as well as to the imposed hydraulic head given by the Dirichlet boundary conditions.

Again, by inverting the matrix $\mathbf{B_K}$ in (14) and using (18b), we eliminate the flux unknowns in (17). We get:

$$\mathbf{R_{in}^T}\,\mathbf{P} - \begin{pmatrix} \mathbf{M_{in}} & \mathbf{M_m} \end{pmatrix} \begin{pmatrix} \mathbf{\Lambda_{in}} \\ \mathbf{\Lambda_m} \end{pmatrix} + \mathbf{V_{in}} = \mathbf{0}, \tag{20}$$

where $\mathbf{R_{in}}$ is a sparse matrix of dimension $card(\mathcal{T}_h)$x$card(\mathcal{E}_{h,in})$, $\mathbf{M_{in}}$ is a sparse matrix of dimension $card(\mathcal{E}_{h,in})$x$card(\mathcal{E}_{h,in})$, $\mathbf{M_m}$ is a sparse matrix of dimension $card(\mathcal{E}_{h,in})$x$card(\mathcal{E}_{h,\Sigma})$ and $\mathbf{V_{in}}$ is a $card(\mathcal{E}_{h,in})$-dimensional vector corresponding to the Dirichlet and Neumann Boundary conditions.

Following the same procedure in condition (18a), we get:

$$\mathbf{R_m^T}\,\mathbf{P} - \begin{pmatrix} \mathbf{M_m^T} & \mathbf{B_m} \end{pmatrix} \begin{pmatrix} \mathbf{\Lambda_{in}} \\ \mathbf{\Lambda_m} \end{pmatrix} + \mathbf{V_m} = \mathbf{0}, \tag{21}$$

with $\mathbf{R_m}$ a sparse matrix of dimension $card(\mathcal{T}_h)$x$card(\mathcal{E}_{h,\Sigma})$, $\mathbf{B_m}$ a square matrix of dimension $card(\mathcal{E}_{h,\Sigma})$x$card(\mathcal{E}_{h,\Sigma})$ and $\mathbf{V_m}$ is a $card(\mathcal{E}_{h,\Sigma})$-dimensional vector corresponding to the Dirichlet Boundary conditions.

Finally, we obtain the following system:

$$\begin{cases} \mathbf{D}\,\mathbf{P} - \begin{pmatrix} \mathbf{R_{in}} & \mathbf{R_m} \end{pmatrix} \begin{pmatrix} \mathbf{\Lambda_{in}} \\ \mathbf{\Lambda_m} \end{pmatrix} & = & \mathbf{F}, \\ \\ \begin{pmatrix} \mathbf{M_{in}} & \mathbf{M_m} \\ \mathbf{M_m^T} & \mathbf{B_m} \end{pmatrix} \begin{pmatrix} \mathbf{\Lambda_{in}} \\ \mathbf{\Lambda_m} \end{pmatrix} - \begin{pmatrix} \mathbf{R_{in}^T} \\ \mathbf{R_m^T} \end{pmatrix} \mathbf{P} - \begin{pmatrix} \mathbf{V_{in}} \\ \mathbf{V_m} \end{pmatrix} & = & 0. \end{cases} \tag{22}$$

We use the notations:

$$\mathbf{M} = \begin{pmatrix} \mathbf{M_{in}} & \mathbf{M_m} \\ \mathbf{M_m^T} & \mathbf{B_m} \end{pmatrix}, \quad \mathbf{\Lambda} = \begin{pmatrix} \mathbf{\Lambda_{in}} \\ \mathbf{\Lambda_m} \end{pmatrix}, \quad \mathbf{V} = \begin{pmatrix} \mathbf{V_{in}} \\ \mathbf{V_m} \end{pmatrix}, \quad \mathbf{R} = \begin{pmatrix} \mathbf{R_{in}} & \mathbf{R_m} \end{pmatrix} \tag{23}$$

Proposition 3.1 *Assuming the transmissivity is locally symmetric positive definite, the matrix*

$$\mathcal{J} = \begin{pmatrix} \mathbf{D} & -\mathbf{R} \\ \\ -\mathbf{R}^T & \mathbf{M} \end{pmatrix} \tag{24}$$

is symmetric and positive definite with the presence of Dirichlet boundary conditions within at least one fracture.

Proof 3.1 *For any non zero vector* $\begin{pmatrix} \mathbf{P} \\ \mathbf{\Lambda_{in}} \\ \mathbf{\Lambda_m} \end{pmatrix}$ *of size* $card(\mathcal{T}_h)xcard(\mathcal{E}_{h,in})xcard(\mathcal{E}_{h,\Sigma})$, *we have*

$$\begin{aligned}
&\begin{pmatrix} \mathbf{P}^T & \mathbf{\Lambda_{in}^T} & \mathbf{\Lambda_m^T} \end{pmatrix} \mathcal{J} \begin{pmatrix} \mathbf{P} \\ \mathbf{\Lambda_{in}} \\ \mathbf{\Lambda_m} \end{pmatrix} \\
&= \mathbf{P}^T\mathbf{D}\mathbf{P} - 2\mathbf{P^T}\mathbf{R_{in}}\mathbf{\Lambda_{in}} - \mathbf{2P^T}\mathbf{R_m}\mathbf{\Lambda_m} \\
&+ \mathbf{\Lambda_{in}^T}\mathbf{M_{in}}\mathbf{\Lambda_{in}} + \mathbf{\Lambda_{in}^T}\mathbf{M_m}\mathbf{\Lambda_m} \\
&+ \mathbf{\Lambda_m^T}\mathbf{M_m}^\mathbf{T}\mathbf{\Lambda_{in}} + \mathbf{\Lambda_m^T}\mathbf{B_m}\mathbf{\Lambda_m} \\
&= \sum_{f=1}^{N_f} \left(\mathbf{\Lambda_f^T}\mathbf{M_f}\mathbf{\Lambda_f} + \mathbf{P_f^T}\mathbf{D_f}\mathbf{P_f} - \mathbf{2P_f^T}\mathbf{R_f}\mathbf{\Lambda_f}\right) \\
&= \sum_{f=1}^{N_f} \begin{pmatrix} \mathbf{P}_f^T & \mathbf{\Lambda_f^T} \end{pmatrix} \mathcal{J}_\mathbf{f} \begin{pmatrix} \mathbf{P}_f \\ \mathbf{\Lambda_f} \end{pmatrix},
\end{aligned} \tag{25}$$

with $\mathbf{M}_f$, $\mathbf{D}_f$ *and* $\mathbf{R}_f$ *the matrices containing the contributions associated to the triangles* K *in* $\mathcal{T}_{h,f}$ *and*

$$\mathcal{J}_\mathbf{f} = \begin{pmatrix} \mathbf{D}_f & -\mathbf{R}_f \\ -\mathbf{R}_f^T & \mathbf{M}_f \end{pmatrix} \tag{26}$$

We get a system within each fracture involving the matrix $\mathcal{J}_\mathbf{f}$ *which is positive definite in presence of Dirichlet boundary conditions and provided the transmissivity is locally symmetric positive definite [7]. At least, one fracture must have Dirichlet boundary conditions to satisfy the property for the matrix* $\mathcal{J}$.

To solve the system, the Schur complement matrix $\mathbf{S} = \mathbf{M} - \mathbf{R}^T\,\mathbf{D}^{-1}\,\mathbf{R}$ is computed and the Schur complement system becomes

$$\begin{cases} \mathbf{S}\,\mathbf{\Lambda} = \mathbf{R^T}\,\mathbf{D^{-1}}\,\mathbf{F} + \mathbf{V}, \\ \mathbf{D}\,\mathbf{P} = \mathbf{R}\,\mathbf{\Lambda} + \mathbf{F}. \end{cases} \tag{27}$$

Using the positive definiteness of $\mathcal{J}$, $\mathbf{S}$ is proved to be positive definite in presence of Dirichlet Boundary conditions. After solving the linear system in $\mathbf{\Lambda}$, the cell hydraulic head $\mathbf{P}$ is derived from the second equation in (27). Finally the three dimensional vector $\mathbf{Q_K}$ containing the fluxes $q_{K,E_i}, i = 1, 2, 3$ on each triangle $K \in \mathcal{T}_h$, are derived using (14), for each $K \in \mathcal{T}_h$.

4 Non-matching grids and mixed hybrid formulation with mortar conditions

The MHFEM described above assumes matching grids at the intersections between fractures.

We suppose now that, for each fracture f, the border $\partial\Omega_f$ is discretized with a mesh step that may be different from the one chosen for the other fractures. Based on this discretization, a 2D mesh is built within each fracture f. An important feature is that now, a given intersection may have a different discretization from one fracture to another.

We make the following assumption:

$$\forall (k_1, k_2), \Sigma_{k_1} \cap \Sigma_{k_2} = \emptyset, \tag{28}$$

that is, we suppose that intersections do not cross nor overlap. Then each intersection Σ_k involves only two fractures. Then for each index k, one associates a unique couple $(f, f^{'})$ of fracture numbers. For each intersection Σ_k, we choose one fracture that is master for this intersection and the other one will be slave. Without loss of generality, suppose f is master for the intersection Σ_k and $f^{'}$ is slave. Notice a fracture may contain some intersections for which it is master and other intersections for which it is slave. We now denote a so-called master discretization $\Sigma_{k,m}$ that is the discretization of Σ_k within the fracture f and a slave discretization $\Sigma_{k,s}$, discretization of Σ_k within the fracture $f^{'}$. In the following, we will use the subscript s to refer to the slave side and m to the master side. We denote by $N_{k,m}$ (respectively $N_{k,s}$) the number of edges in $\Sigma_{k,m}$ (respectively $\Sigma_{k,s}$) and $N_s = \sum_{k=1}^{N_i} N_{k,s}$, $N_m = \sum_{k=1}^{N_i} N_{k,m}$.

4.1 Mixed hybrid formulation with mortar conditions

The weak formulation in case of non-matching grids includes equations $(7a-7c)$ but equations at intersections have to be rewritten to ensure the continuity of the fluxes and hydraulic heads at the non-matching intersections. Here we do not introduce another unknown for the intersection trace because each intersection involves only two fractures.

We need the following spaces:

$$\begin{aligned} \mathcal{N}^0(\Sigma_{k,m}) &= \{\mu_h \in L^2(\Sigma_k), \text{ such that } \mu_h \in P^0(E), \forall E \in \Sigma_{k,m}\} \\ \mathcal{N}^0(\Sigma_{k,s}) &= \{\mu_h \in L^2(\Sigma_k), \text{ such that } \mu_h \in P^0(E), \forall E \in \Sigma_{k,s}\}. \end{aligned} \tag{29}$$

The continuity of the flux for each intersection Σ_k writes:

$$\sum_{\substack{K \in \mathcal{T}_{h,f},\\ meas(\partial K \cap \Sigma_k) \neq 0}} \int_{\partial K \cap \Sigma_k} \mathbf{u}_{h,f}.\boldsymbol{\nu}_{K,f}\mu_h dl + \sum_{\substack{K^{'} \in \mathcal{T}_{h,f'},\\ meas(\partial K^{'} \cap \Sigma_k) \neq 0}} \int_{\partial K^{'} \cap \Sigma_k} \mathbf{u}_{h,f'}.\boldsymbol{\nu}_{K',f'}\mu_h dl = 0,\ \forall \mu_h \in \mathcal{N}^0(\Sigma_{k,m}). \tag{30}$$

The continuity of the hydraulic head for each intersection Σ_k writes:

$$\int_{\Sigma_{k,s}} \lambda_{h,f'}\mu_h dl = \int_{\Sigma_{k,m}} \lambda_{h,f}\mu_h dl, \forall \mu_h \in \mathcal{N}^0(\Sigma_{k,s}), \tag{31}$$

which defines the L^2 projection from the master side to the slave side.

4.2 Derivation of the linear system

We still denote by $\mathbf{P_f}$ the vector of cell hydraulic head for all K in $\mathcal{T}_{h,f}$, $\mathbf{P} = (\mathbf{P_f})_\mathbf{f}$ and by $\mathbf{\Lambda_f}$ the vector of trace of hydraulic head unknowns $\lambda_{E,f}$ on edges in $\mathcal{E}_{h,f}$.

Relations (14) and (17) stay the same.

Since the meshes do not coincide at the intersections, the interface conditions (18a) and (18b) have to be rewritten. On an intersection $\Sigma_k = \bar{\Omega}_f \cap \bar{\Omega}_{f'}$, (with f the master fracture and $f^{'}$ the slave one for Σ_k), we define $(Q_{E,f})_{E\in\Sigma_{k,m}}$ (respectively $(Q_{E,f'})_{E\in\Sigma_{k,s}}$) the vector of jump of flux through the edges of $\Sigma_{k,m}$ (respectively $\Sigma_{k,s}$). Relations (30) and (31) write:

$$(Q_{E,f})_{E\in\Sigma_{k,m}} + \mathbf{C_k}^T (Q_{E,f'})_{E\in\Sigma_{k,s}} = \mathbf{0}, \tag{32a}$$

$$(\lambda_{E,f'})_{E\in\Sigma_{k,s}} = \mathbf{C_k}(\lambda_{E,f})_{E\in\Sigma_{k,m}}, \tag{32b}$$

with $\mathbf{C_k}$ a matrix of size $N_{k,s}$x$N_{k,m}$ that represents the L^2-projection from the master side to the slave side. Its coefficients C_{ln}, $l \in \{1, ..., N_{k,s}\}$, $n \in \{1, ..., N_{k,m}\}$, are the ratio between the intersection lengths of a slave edge E_l and a master edge E_n and over the length of E_l:

$$C_{ln} \quad = \quad \left(\frac{|E_n \cap E_l|}{|E_l|} \right), \tag{33}$$

where the notation $|E|$ stands for the length of the edge E.

We define the matrix $\mathbf{C}$ as an intersection-block matrix with blocks (C_k).

On a fracture f, we distinguish inner edges, slave edges and master edges, so that the trace of hydraulic head unknowns form a vector

$$\mathbf{\Lambda_f} = \begin{pmatrix} \mathbf{\Lambda_{in,f}} \\ \mathbf{\Lambda_{m,f}} \\ \mathbf{\Lambda_{s,f}} \end{pmatrix} \tag{34}$$

We define also two global variables $\mathbf{\Lambda_m} = (\mathbf{\Lambda_{m,f}})_\mathbf{f}$ and $\mathbf{\Lambda_s} = (\mathbf{\Lambda_{s,f}})_\mathbf{f}$.

We substitute $\mathbf{\Lambda_{m,f}}$, $\mathbf{\Lambda_{s,f}}$ and $\mathbf{\Lambda_{in,f}}$ by their equivalent global unknowns $\mathbf{\Lambda_m}$, $\mathbf{\Lambda_s}$ and $\mathbf{\Lambda_{in}}$ respectively.

Using (32b), we have the following relation:

$$\mathbf{\Lambda_s} = \mathbf{C}\mathbf{\Lambda_m}. \tag{35}$$

The mass conservation equations (7b) are written by inverting $\mathbf{B_K}$ in (14) and using (35):

$$\mathbf{D\,P} - \begin{pmatrix} \mathbf{R_{in}} & \mathbf{R_m} + \mathbf{R_s C} \end{pmatrix} \begin{pmatrix} \mathbf{\Lambda_{in}} \\ \mathbf{\Lambda_m} \end{pmatrix} = \mathbf{F} \tag{36}$$

Also, by inverting the matrix $\mathbf{B_K}$ in (14), we eliminate the flux unknowns in (17). Using (35), we eliminate $\mathbf{\Lambda_s}$, yielding:

$$\mathbf{R_{in}^T\,P} - \begin{pmatrix} \mathbf{M_{in}} & \mathbf{M_m} + \mathbf{M_s C} \end{pmatrix} \begin{pmatrix} \mathbf{\Lambda_{in}} \\ \mathbf{\Lambda_m} \end{pmatrix} + \mathbf{V_{in}} = \mathbf{0}, \tag{37}$$

where $\mathbf{R_{in}}$ is a sparse matrix of dimension $card(\mathcal{T}_h)$x$card(\mathcal{E}_{h,in})$ and $\mathbf{M_{in}}$ a sparse matrix of dimension $card(\mathcal{E}_{h,in})$x$card(\mathcal{E}_{h,in})$, $\mathbf{M_m}$ of dimension $card(\mathcal{E}_{h,in})$xN_m, $\mathbf{M_s}$ of dimension $card(\mathcal{E}_{h,in})$xN_s and $\mathbf{C}$ is of dimension N_sxN_m .

Following the same procedure in condition (32a), one has:

$$(\mathbf{R_m^T} + \mathbf{C}^T\mathbf{R_s^T})\,\mathbf{P} - \begin{pmatrix} \mathbf{M_m^T} + \mathbf{C}^T\mathbf{M_s^T} & \mathbf{B_m} + \mathbf{C}^T\mathbf{B_s C} \end{pmatrix} \begin{pmatrix} \mathbf{\Lambda_{in}} \\ \mathbf{\Lambda_m} \end{pmatrix} + \mathbf{V_m} = \mathbf{0}. \tag{38}$$

with $\mathbf{R_m}$ a sparse matrix of dimension $card(\mathcal{T}_h)$xN_m, $\mathbf{R_s}$ a sparse matrix of dimension $card(\mathcal{T}_h)$xN_s, $\mathbf{B_s}$ a square matrix of dimension N_sxN_s and $\mathbf{B_m}$ a square matrix of dimension N_mxN_m.

The system takes the form:

$$\begin{cases} \mathbf{D\,P} - \begin{pmatrix} \mathbf{R_{in}} & \mathbf{R_m} + \mathbf{R_s C} \end{pmatrix} \begin{pmatrix} \mathbf{\Lambda_{in}} \\ \mathbf{\Lambda_m} \end{pmatrix} & = & \mathbf{F}, \\ \begin{pmatrix} \mathbf{M_{in}} & \mathbf{M_m} + \mathbf{M_s C} \\ \mathbf{M_m^T} + \mathbf{C}^T\mathbf{M_s^T} & \mathbf{B_m} + \mathbf{C}^T\mathbf{B_s C} \end{pmatrix} \begin{pmatrix} \mathbf{\Lambda_{in}} \\ \mathbf{\Lambda_m} \end{pmatrix} - \begin{pmatrix} \mathbf{R_{in}^T} \\ \mathbf{R_m^T} + \mathbf{C}^T\mathbf{R_s^T} \end{pmatrix} \mathbf{P} - \mathbf{V} & = & 0. \end{cases} \tag{39}$$

Let us take the same notations as in (23):

$$\mathbf{M} = \begin{pmatrix} \mathbf{M_{in}} & \mathbf{M_m} + \mathbf{M_s C} \\ \mathbf{M_m}^T + \mathbf{C}^T \mathbf{M_s}^T & \mathbf{B_m} + \mathbf{C}^T \mathbf{B_s C} \end{pmatrix},$$
$$\mathbf{\Lambda} = \begin{pmatrix} \mathbf{\Lambda_{in}} \\ \mathbf{\Lambda_m} \end{pmatrix}, \mathbf{R} = \begin{pmatrix} \mathbf{R_{in}} & \mathbf{R_m} + \mathbf{R_s C} \end{pmatrix}. \tag{40}$$

then we find a system of the same form as before.

Proposition 4.1 *Assuming the transmissivity is locally symmetric positive definite, the matrix*

$$\mathcal{J} = \begin{pmatrix} \mathbf{D} & -\mathbf{R} \\ -\mathbf{R}^T & \mathbf{M} \end{pmatrix} \tag{41}$$

is symmetric and, with the presence of Dirichlet boundary conditions within at least one fracture, it is positive definite.

Proof 4.1 *The proof is similar to the one presented for the matching grids case. We use relation* (35) *to introduce* $\mathbf{\Lambda_s}$ *and to identify* $\mathbf{\Lambda_f}$ *in the expression.*

For any non zero vector $\begin{pmatrix} \mathbf{P} \\ \mathbf{\Lambda_{in}} \\ \mathbf{\Lambda_m} \end{pmatrix}$ *of size* $card(\mathcal{T}_h) x card(\mathcal{E}_{h,in}) x N_m$*, we have*

$$\begin{aligned} \begin{pmatrix} \mathbf{P}^T & \mathbf{\Lambda_{in}^T} & \mathbf{\Lambda_m^T} \end{pmatrix} \mathcal{J} \begin{pmatrix} \mathbf{P} \\ \mathbf{\Lambda_{in}} \\ \mathbf{\Lambda_m} \end{pmatrix} &= \mathbf{P}^T \mathbf{D} \mathbf{P} - 2\mathbf{P^T R_{in} \Lambda_{in}} - \mathbf{2 P^T R_m \Lambda_m} - \mathbf{2\, P^T R_s \Lambda_s} \\ &\quad + \mathbf{\Lambda_{in}^T M_{in} \Lambda_{in}} + \mathbf{\Lambda_{in}^T M_m \Lambda_m} + \mathbf{\Lambda_{in}^T M_s \Lambda_s} \\ &\quad + \mathbf{\Lambda_m^T M_m}^{\mathbf{T}} \mathbf{\Lambda_{in}} + \mathbf{\Lambda_s^T M_s}^{\mathbf{T}} \mathbf{\Lambda_{in}} \\ &\quad + \mathbf{\Lambda_m^T B_m \Lambda_m} + \mathbf{\Lambda_s^T B_s \Lambda_s} \\ &= \sum_{f=1}^{N_f} \left(\mathbf{\Lambda_f^T M_f \Lambda_f} + \mathbf{P_f^T D_f P_f} - \mathbf{2 P_f^T R_f \Lambda_f} \right), \end{aligned} \tag{42}$$

with $\mathbf{M}_f$*,* $\mathbf{D}_f$ *and* $\mathbf{R}_f$ *the matrices containing the contribution associated to the triangles* K *within the fracture* f*.*

Then, we conclude by a same argument as in Proposition (3.1)*.*

5 Numerical simulations

We consider a discrete fracture network embedded in a cube of edge size 100 m and assume that the following boundary conditions hold on the cube sides:

- Imposed Dirichlet Boundary Condition on the top and bottom sides of the cube (Imposed hydraulic head of value 10m on top and 0m on bottom)
- Null flux on the lateral side of the cube,

We consider the geometry given on figure 2 (left) with 15 fractures and 85 intersections. Notice the preferential orientation of the fractures with respect to the boundary conditions since for any vertical 2D slice, the associated 2D network is given on figure 2 (right). For this 2D network, the solution is easily derived at the intersection points and is the reference for the comparison with the 3D computations. Indeed, due to this preferential orientation of the fractures in 3D, one can compute the solution for the 3D network, then extract all the values obtained on the intersection lines. For each intersection Σ_k, we compute the relative error e_k between the values obtained in 3D and the corresponding value in 2D. Once those relative errors are computed for each intersection, the global mean relative error on the intersections is: $e = \frac{1}{N_i} \sum_{k=1}^{N_i} e_k$

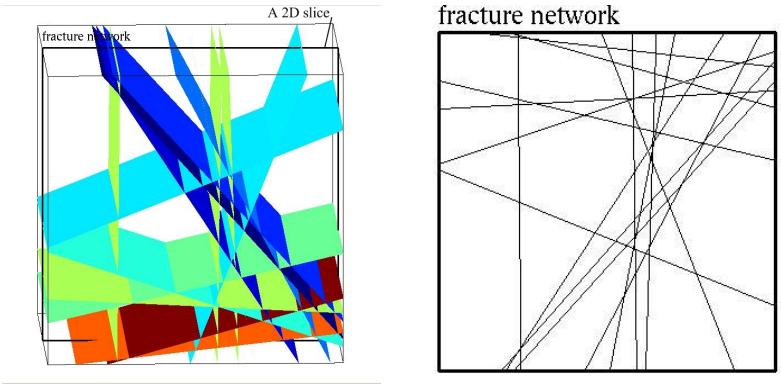

Figure 2: Geometry of the intersecting fractures and an associated 2D slice

We take the transmissivity tensor as equal to $\mathcal{T} = \begin{pmatrix} 10^{-3} & 0 \\ 0 & 10^{-3} \end{pmatrix}$ $\mathrm{m}^2.\mathrm{s}^{-1}$. It corresponds to a fracture aperture of 1.07 mm (for water at 20 $^\circ$C).

We perform simulations for two different meshes of the domain:

- With matching grids at the intersections and a total edges number of 33,164 with a mesh step of 10m,

- With non-matching grids at the intersections and a total edges number of 23,362 with mesh steps ranging from 3m to 8m.

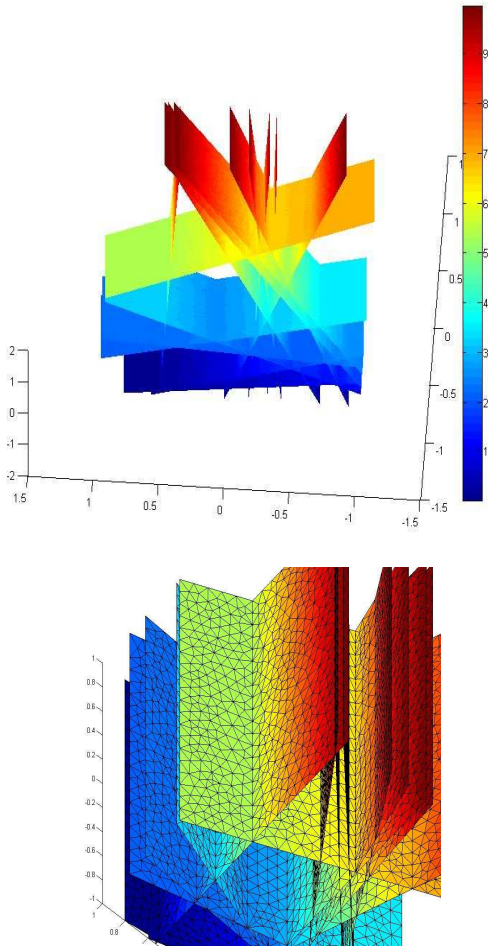

Figure 3: Mean hydraulic head for the matching grids case and zoom on the mesh

On figure 3, the mean hydraulic head is shown for the matching grids case. On the figures, the space scale is adimensionalised. The expected solution is obtained with a global mean relative error e of $4.25\text{x}10^{-6}$ by comparison with the 2D case. The input flux is equal to $0.08\text{m}^3.\text{s}^{-1}$. The equivalent permeability defined as the ratio between the input flux over the product of the domain length by $\Delta h = 10$ is equal to $8.04\text{x}10^{-5}\text{m.s}^{-1}$. We also verify that the method does not create any artificial flux at the intersections by summing all the fluxes on

intersections, which gives $3\text{x}10^{-13}\text{m}^3.\text{s}^{-1}$.

For the non-matching grids case (figure 4), the global mean relative error e obtained by comparison with the 2D case is equal to $4.25\text{x}10^{-6}$. The input flux is equal to $0.08\text{m}^3.\text{s}^{-1}$. The equivalent permeability is equal to $8.04\text{x}10^{-5}\text{m}.\text{s}^{-1}$. The sum of the fluxes on intersections is equal to $4\text{x}10^{-13}\text{m}^3.\text{s}^{-1}$. Results are in agreement with what are obtained in the 2D case and with the matching grids case.

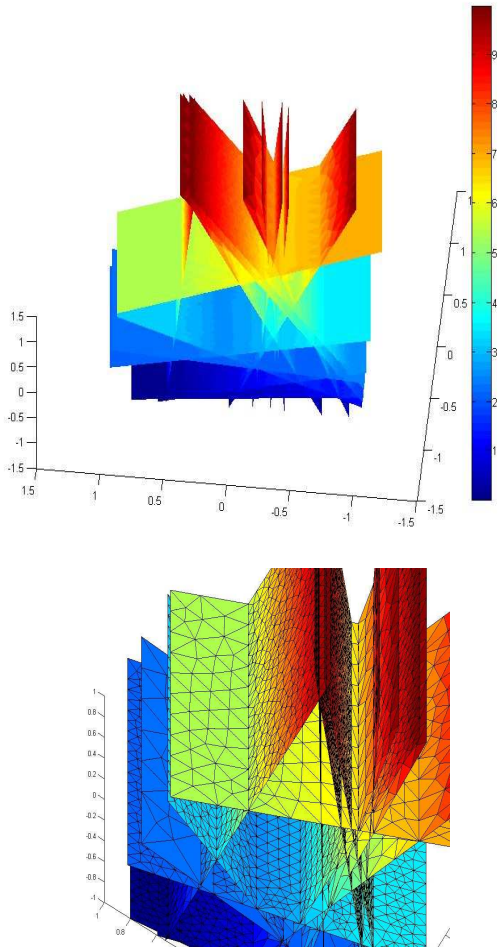

Figure 4: Mean hydraulic head for the non-matching grids case and zoom on the mesh

6 Conclusion

This article describes a mortar method combined with a mixed hybrid finite element method applied to simulate flow in Discrete Fracture Networks. This allows to generate non-matching grids in each fracture. We propose an algebraic formulation of the mortar conditions to eliminate the flux unknowns, leading to a Schur complement system of the same form as in the MHFEM with matching grids at the intersections. Our numerical experiments show a good agreement between matching and non matching grids. The method assumes that intersections do not cross nor overlap, so that each intersection involves exactly two fractures. The adaptation of the method for more general networks will be presented in a forthcoming paper.

Acknowledgement

We sincerely wish to thank the reviewers for their constructive comments. This work was supported by the French National Research Agency, with the ANR-07-CIS-004 project MICAS.

References

[1] J.-R. de Dreuzy, P. Davy, O. Bour, *Permeability of 2D fracture networks with power law distributions of length and aperture*,Water Resources Research, 38, pp. 1-9, 2002.

[2] J. Erhel, J.- R. de Dreuzy, B. Poirriez, *Flow simulation in three-dimensional discrete fracture network* , SIAM Journal on Scientific Computing, Vol. 31, No. 4, pp. 2688-2705, 2009.

[3] C. Bernardi, Y. Maday and A. T. Patera, *Domain decomposition by the Mortar element method*, Asymptotic and numerical methods for partial differential equations with critical parameters (Beaune, 1992),editors: H.G. Kaper & M. Garbey, N.A.T.O. ASI Series C 384, pp. 269-286, Kluwer Acad. Publ., Dordrecht, 1993.

[4] C. Bernardi, Y. Maday and A. T. Patera, *A new conforming approach to domain decomposition: the mortar element method*,Nonlinear partial differential equations and their applications, Collège de France Seminar, Vol. XI (Paris, 1989-1991), pp. 13-51, Longman Sci. Tech., Harlow, 1994.

[5] C. Bernardi and Y. Maday, *Spectral, spectral element and mortar element method*, Theory and numerics of differential equations (Durham, 2000), pp. 1-57. Springer, Berlin, 2001.

[6] T. Arbogast, L. C. Cowsar, M. F. Wheeler, I. Yotov, *Mixed finite element methods on non-matching multiblock grids*, SIAM J. Numer. Anal., 37(4), pp. 1295-1315, 2000.

[7] H. Hoteit, J. Erhel, R. Mosé, B. Philippe and Ph. Ackerer. *Numerical reliability for mixed methods applied to flow problems in porous media*, Computational Geosciences, 6, pp. 161-194, 2002.

[8] H. Hoteit, *Simulation d'écoulements et de transports de polluants en milieux poreux :Application à la modélisation de la sûreté des dépôts de déchets radioactifs*, PhD Rennes1 University, 2002.

[9] D. N. Arnold and F. Brezzi *Mixed and nonconforming finite element methods: implementation, post-processing and error estimates*, Mathematical Modelling and Numerical Analysis, 19(1), pp. 7-32, 1985.

[10] J. Jaffré, V. Martin, J. E. Roberts, *Modeling fractures and barriers as interfaces for flow in porous media*, SIAM J. Sci. Comput., Vol. 26 (5), pp. 16671691, 2005.

[11] M. Vohralik, *Méthodes numériques pour des équations elliptiques et paraboliques non linéaires, Application à des problèmes d'écoulement en milieux poreux et fracturés*, PhD Paris IX Orsay University and Czech Technical University in Prague, 2004.